Structure and Properties of Polyfluoride F n − Clusters (n = 3−29)

ARTICLE *in* THE JOURNAL OF PHYSICAL CHEMISTRY A · MAY 2015

Impact Factor: 2.69 · DOI: 10.1021/acs.jpca.5b02431 · Source: PubMed

6 AUTHORS, INCLUDING:

K.G. Belay
Florida A&M University
17 PUBLICATIONS **91** CITATIONS
SEE PROFILE

Charles Weatherford
Florida A&M University
119 PUBLICATIONS **457** CITATIONS
SEE PROFILE

B. R. Ramachandran
Louisiana Tech University
62 PUBLICATIONS **576** CITATIONS
SEE PROFILE

L.G. Gutsev
Florida State University
8 PUBLICATIONS **6** CITATIONS
SEE PROFILE

THE JOURNAL OF PHYSICAL CHEMISTRY A

Article

pubs.acs.org/JPCA

Structure and Properties of Polyfluoride F_n^- Clusters (n = 3−29)

G. L. Gutsev,*[,†] K. G. Belay,[†] C. A. Weatherford,[†] B. R. Ramachandran,[‡] L. G. Gutsev,[§] and P. Jena[∥]

[†]Department of Physics, Florida A&M University, Tallahassee, Florida 32307, United States

[‡]College of Engineering & Science, Louisiana Tech University, Ruston, Louisiana 71272, United States

[§]Department of Chemistry and Biochemistry, Florida State University, Tallahassee, Florida 32306,United States

[∥]Department of Physics, Virginia Commonwealth University, Richmond, Virginia 23284, United States

ABSTRACT: The electronic and geometrical structures of the neutral F_n and singly negatively charged F_n^- polyfluorides (n = 3−29) are studied using three levels of theory: density functional theory (DFT) with generalized gradient approximation, hybrid Hartree−Fock-DFT, and hybrid HF-DFT with long-range corrections. For $n > 4$, each polyfluoride possesses a number of states with different geometries that are closely spaced in total energy. The geometrical structures of the lowest total energy states follow different patterns for the even-n and odd-n F_n^- anion branches with a preference for higher symmetry geometries. The largest F_{29}^- anion considered is found to possess O_h symmetry. All the anions beginning with F_3^- are found to possess adiabatic and vertical electron detachment energies exceeding the electron affinities of halogen atoms and are therefore superhalogen anions. Electron affinities, energies of formation, and binding energies show oscillatory behavior as functions of the number n of fluorine atoms. The neutral F_n species are found to be barely stable and are bound by polarization forces. The F_n^- anions, on the contrary, are quite stable toward the loss of F, F^-, and F_2^-, but not to the loss of F_2.

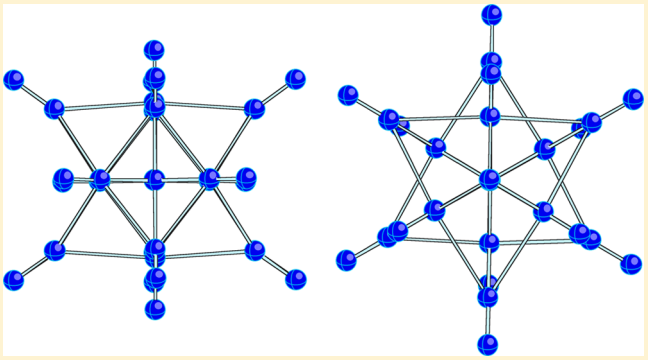

1. INTRODUCTION

The structure and chemistry of polyhalides are intriguing subjects and have attracted considerable attention.[1] Among polyhalides, the most studied systems are polyiodides, which exist in salts in a great variety of quasi-linear chains, two- and three-dimensional networks as well as single clusters.[2] The largest single iodine cluster observed appears to be a nonacosaiodide I_{29}^{3-} cluster in the $[Fe(C_5H_5)_2]_3I_{29}$ salt.[3] The I_n^- anions have been theoretically studied[4] for odd n = 3, 5, and 7, and the results support the conclusion that these anions are composed of I_2 and linear I_3 units. A joint experimental and theoretical study[5] performed for I_n^- in the range $2 \le n \le 15$ showed that the branched geometrical structures of the I_n^- anions are strongly favored.

Polybromides are less studied than polyiodides. They are found to be capable of forming 2D- and 3D-networks in chemical compounds[6−8] and can also exist as separate clusters such as Br_9^- ions of T_d symmetry[9,10] or Br_{11}^- ions of D_{3h} symmetry.[11] The next series of the polyhalides family, polychlorides, are studied in even less detail than polybromides. Experimental investigations have dealt mainly with the salts containing Cl_3^- and Cl_5^- anions[12] whereas theoretical computations have been performed for the Cl_n^- anions (n = 3−7)[13,14] using density functional theory and coupled cluster theory for the Cl_n^- anions (n = 3, 5, 7, and 9)[15] and the Cl_4^+ cation. Gas-phase experimental studies[17] have been performed for I_3^-, Br_3^-, and Cl_3^- anions, and the anions' dissociation energies and electron affinities of the corresponding neutral parents have been estimated. Both singly positively and negatively charged species X_n (X = Cl, Br, and I; n = 3−5) have been investigated[18] using coupled cluster theory. It is curious that trichloride, tribromide, triiodine, and pentabromine can serve[19] as positively charged counterions in salts $[polyhalide]^+[AsF_6]^-$, where the AsF_6 is a classic superhalogen.[20]

Polyfluorides are studied to a lesser extent[21] than polybromides and polychlorides. Only the F_3^- anion is shown on a diagram displaying all experimentally observed polyhalide anions in a recent review by Haller and Riedel.[1] This anion had attracted a lot of attention from theoreticians[22−31] before having been observed by Compton et al.,[32] although exhaustive attempts to synthesize a $[N(CH_3)_4]^+F_3^-$ salt were unsuccessful.[33]

According to the results of computations, the F_3^- anion possesses a strong multireference[34] character and a four-electron three-center (4e, 3c) bond.[35,36] Excited states of the F_3^- anion have been probed using the internally contracted configuration interaction method, and only a single bound excited state possessing an angular geometrical structure was

Received: March 12, 2015
Revised: May 12, 2015
Published: May 14, 2015

DOI: 10.1021/acs.jpca.5b02431
J. Phys. Chem. A 2015, 119, 6483−6492

Table 1. Electron Affinity of F and Adiabatic Electron Affinity of F_2 and F_3 Computed by Using Different Methods[a]

		F		F_2		F_3	
method		6-311+G*	6-311+G(3df)	6-311+G*	6-311+G(3df)	6-311+G*	6-311+G(3df)
DFT	BPW91	3.55	3.52	3.80	3.58	5.52	5.39
	PBE	3.58	3.54	3.79	3.55	5.56	5.37
	PKZB	3.19	3.19	3.60	3.67	5.13	4.86
	TPSS	3.36	3.36	3.70	3.48	5.41	5.17
	revTPSS	3.32	3.29	3.62	3.39	5.34	5.10
HF-DFT	B3LYP	3.49	3.46	3.96	3.73	5.06	4.89
	B3PW91	3.36	3.36	3.80	3.55	4.89	4.69
long range corrected	LC-ωPBE	3.50	3.47	3.75	3.47	4.49	4.31
	ωB97XG	3.38	3.35	3.66	3.49	4.61	4.42
	CAM-B3LYP	3.50	3.47	3.88	3.63	4.81	4.58
double	B2PLYP	3.30	3.36	3.60	3.43	4.97	4.85
post-HF	CCSD(T)	3.00	3.33	2.97	3.00	4.14	4.28
experiment		3.399 ± 0.003[b]		3.08 ± 0.1[e]			
		3.401188 ± 0.000032[c,d]		3.01 ± 0.07[f]			

[a]All values are in eV. [b]See ref 69. [c]See ref 70. [d]See ref 71. [e]See ref 72. [f]See ref 73.

identified.[37] Among other polyfluorides, only F_4^- and F_5^- have been computed at different levels of theory.[38]

This work presents a computational study of the structures and properties of the neutral F_n and F_n^- anions (n = 3−29) that correspond to the lowest total energy states correspond to the lowest total energy states. To the best of our knowledge, it is the first computational study of these species for n > 5. The value of 29 was chosen because it corresponds to the largest polyiodide ion I_{29}^{3-} known. Both F_2^- and F_3^- possess relatively large adiabatic and vertical energies associated with an extra electron detachment. One can anticipate that the same holds for larger polyfluoride anions; therefore, we have computed adiabatic and vertical electron detachment energies for the F_n^- anions with n > 3. Of special interest is the question whether the F_n^- anions are stable for n > 5. The energies of dissociation via different decay channels have been estimated for the lowest total energy states of the F_n^- anions to make sure that these states are stable with respect to dissociation. For understanding the nature of bonding in the anions, we have plotted valence molecular orbitals for selected anions.

2. CALIBRATION OF COMPUTATIONAL APPROACHES

To gain insight into the dependence of computational results on the basis and method used, we performed calibration calculations for F, F_2, F_3, F^-, F_2^-, and F_3^- using the 6-311+G* basis of triple-ζ quality and its 6-311+G(3df) extension[39] combined with 12 methods belonging to different groups. In our selection, density functional theory (DFT) is represented by the BPW91[40,41] and PBE,[42] methods for the generalized gradient approximation (DFT-GGA) to the exchange−correlation functional and the PZKB,[43] TPSS,[44] and revTPSS[45] methods with the τ-dependent gradient-corrected functional. The hybrid Hartree−Fock-DFT group is presented by the B3LYP,[46] B3PW91, and double hybrid B2PLYP methods,[47] whereas long-range corrected methods are presented by LC-ωPBE,[48−50] CAM-B3LYP,[51] and ωB97XG.[52] Post-HF wave function-based methods are presented by the coupled cluster method with singles and doubles and noniterative inclusion of triples CCSD(T).[53] All our computations are performed using the GAUSSIAN 09 suite of programs.[54]

The geometries of F_2, F_3, and their anions have been optimized at the corresponding level of theory and zero-point vibrational point (ZPVE) energies have been obtained from harmonic vibrational frequency calculations following each geometry optimization. The electron affinity (EA) of a F atom is computed as the difference in total energies between F and F^-, whereas the adiabatic electron affinity (EA_{ad}) of F_2 and F_3 are computed as

$$EA_{ad}(F_n) = [E_{tot}^{el}(F_n) + E_0(F_n)] - [E_{tot}^{el}(F_n^-) + E_0(F_n^-)] \quad (1)$$

where E_{tot}^{el} is the total Born−Oppenheimer energy and E_0 is the zero-point vibrational energy.

The results of our test computations on the electron affinity using all selected methods are presented in Table 1. As can be seen, all computed EA values of the F atom are within ±0.2 eV (6%) of the experimental value. The extension of the 6-311+G* basis set results in the EA changes, which do not exceed 0.06 eV except for the expected larger difference for the values computed using the CCSD(T) method. All methods seriously overestimate the EA_{ad} of F_2 and the basis extension reduces the error by 0.25 eV on average, except for the CCSD(T) method where the computed value matches the experimental values within the experimental error bars. The largest CCSD(T) T_2 amplitude, which accounts for contributions from the states other than the reference state, is 0.14 for F_2 and 0.02 for F_2^-. The T_2 amplitudes for F_3 and F_3^- are 0.14 and 0.16, respectively, which is in agreement with the previously found multireference character of the F_3^- wave function.[34]

Dissociation energies of F_2 and F_2^- have been computed according to the equation

$$D_0(F_2^{0,-} \rightarrow F^{0,-} + F) = E_{tot}^{el}(F^{0,-}) + E_{tot}^{el}(F) - [E_{tot}^{el}(F_2^{0,-}) + E_0(F_2^{0,-})] \quad (2)$$

and dissociation energies of F_3^- as

$$D_0(F_3^- \rightarrow F_2 + F^-) = [E_{tot}^{el}(F_2) + E_0(F_2)] + E_{tot}^{el}(F^-) - [E_{tot}^{el}(F_3^-) + E_0(F_3^-)] \quad (3)$$

and

$$D_0(F_3^- \rightarrow F + F_2^-) = [E_{tot}^{el}(F_2^-) + E_0(F_2^-)] + E_{tot}^{el}(F) - [E_{tot}^{el}(F_3^-) + E_0(F_3^-)] \quad (4)$$

DOI: 10.1021/acs.jpca.5b02431
J. Phys. Chem. A 2015, 119, 6483−6492

Table 2. Comparison of Dissociation Energies of F_2 and F_2^- Computed by Using Different Methods with Experiment[a]

method		$F_2 \rightarrow F + F$		$F_2^- \rightarrow F + F^-$		$F_3^- \rightarrow F_2 + F^-$		$F_3^- \rightarrow F + F_2^-$	
		6-311+G*	6-311+G(3df)	6-311+G*	6-311+G(3df)	6-311+G*	6-311+G(3df)	6-311+G*	6-311+G(3df)
DFT	BPW91	1.85	2.03	2.10	2.10	2.09	1.92	1.84	1.86
	PBE	2.00	2.19	2.21	2.20	2.18	2.00	1.98	2.00
	PKZB	1.56	1.74	1.97	1.96	1.95	1.76	1.54	1.54
	TPSS	1.74	1.91	2.07	2.06	2.09	1.93	1.76	1.78
	revTPSS	1.78	1.96	2.08	2.07	2.09	1.92	1.79	1.81
HF-DFT	B3LYP	1.32	1.51	1.79	1.78	1.62	1.45	1.14	1.18
	B3PW91	1.29	1.50	1.73	1.72	1.53	1.36	1.09	1.14
long range corrected	LC-wPBE	1.30	1.54	1.55	1.54	0.99	0.84	0.75	0.84
	wB97XG	1.26	1.48	1.63	1.62	1.25	1.08	0.88	0.93
	CAM-B3LYP	1.30	1.51	1.68	1.68	1.30	1.15	0.92	0.99
double	B2PLYP	1.18	1.45	1.48	1.51	1.58	1.49	1.34	1.43
post-HF	CCSD(T)	1.19	1.65	1.15	1.32	1.01	1.08	1.19	1.40
experiment		1.58 ± 0.03[b]		1.21 ± 0.07[c]		1.02 ± 0.11[d]		1.30 ± 0.13[d]	

[a]All values are in eV. [b]See ref 74. [c]See ref 57. [d]See ref 75.

The results of computations using all chosen methods and both basis sets are compared with experimental data in Table 2. As can be seen, the values obtained for F_2 are in fair agreement with experiment except for the values obtained using the DFT-GGA methods.

Feller and Peterson[55] have reported dissociation energies for F_2 obtained by extrapolating three series of CCSD(T)/aug-cc-pV*n*Z computations (n = 2−4, 3−5, and 4−6) to the complete basis set limit, and obtained errors of 3.8%, 2.0%, and 1.8%, respectively. The experimental dissociation energy of F_2 contains a fairly large spin−orbit contribution from the $F(^2P)$ atom ground state, which is not represented in our calculations. Feller and Peterson took this effect into account by adjusting the experimental dissociation energy so that theory and experiment could be compared on the same footing. We have not done so and obtained the following errors using the basis set 6-311+G(3df): BPW91, 30%; B3LYP, 5%; CAM-B3LYP, 4%; CCSD(T), 4%.

In the case of F_2^-, agreement is less satisfactory and all methods predict larger values than those obtained from experiment. Note that the computed dissociation energies do not nearly depend on the basis set except for those obtained at the CCSD(T) level of theory. The dissociation energies via the $F_3^- \rightarrow F_2 + F^-$ and $F_3^- \rightarrow F + F_2^-$ decay channels exhibit different patterns as functions of the basis set. The former decrease when the basis increases whereas the latter become slightly larger [except for those obtained using the PKZB and CCSD(T) methods] when the basis set increases.

Computations of larger neutral and singly negatively charged F_n clusters are performed using three methods: BPW91 (the DFT-GGA group), B3LYP (the HFDFT group), and CAM-B3LYP (the long-range corrected HFDFT group) and the 6-311+G* basis set. When selecting these methods, we took into account that the B3LYP and CAM-B3LYP methods showed small root-mean square errors in computations of compounds possessing halogen bonds.[56,57] The BPW91 method was chosen because it is more stable in harmonic vibrational frequency computations[58] than some other DFT-GGA methods. For each anion, we performed a search for its optimal geometric structure using a number of guess structures including branched and saw-chain structures. Geometrical structures used for lowest total energy states of the anions have been used as initial geometries in optimizations of the corresponding neutrals. To confirm the stationary character of a state obtained, each geometry optimization has been followed by harmonic vibrational frequency computations. All the lowest total energy states of F_n and F_n^- are singlets or doublets depending on the charge of a species and its n parity.

3. RESULTS AND DISCUSSION

We will start by discussing the trends in geometrical structures of the lowest total energy states of F_n^- and F_n species. Next, we will present the results of our computations on the electron affinities and ionization energies using the BPW91, B3LYP, and CAM-B3LYP methods followed by a discussion of binding energies of the anions. In particular, we will present the energies corresponding to the loss of F, F^-, F_2, and F_2^-. To gain insight into the molecular structure of the F_n^- anions, we present diagrams of valence molecular orbitals (MO) for selected anions.

3.1. Geometries of Polyfluorides. Geometrical structures corresponding to the lowest total energy states of the F_n and F_n^- species are presented in Figure 1 for n = 2−7. In agreement with the CCSD(T) result,[38] the geometrical structure of F_4^- is linear whereas F_5^- possesses a C_{2v} structure similar to the structures found previously for I_5^-,[4] Br_5^-,[18] and Cl_5^-.[14,15] The F_7^- anion is found to possess a planar D_{3h} structure. Geometries of the lowest total energy states of other polyhalides X_7^- are different: the Cl_7^- and Br_7^- ions have been found to possess[15,59] pyramidal geometrical structures of C_{3v} symmetry whereas I_7^- has been found to possess a zigzag geometrical configuration of C_{2h} symmetry in ref 4 and C_{3v} symmetry in ref 5.

Figure 2 presents the lowest total energy state structures of F_n and F_n^- species for n = 8−12. The lowest total energy state structures of the anions for n = 13−18, 19−24, and 25−29 are presented in Figures 3, 4, and 5, respectively. All polyhalide X_9^- ions have been found to possess tetrahedral geometrical structures similar to the one presented in Figure 2 for the F_9^- anion. It is interesting to note that the polyinterhalide ion ClI_8^- possesses[60] a planar geometrical structure of D_{4h} symmetry. The central atom in F_{11}^- is pentacoordinated and a similar geometrical structure was found for Br_{11}^- in the $[PPN][Br_{11}{\cdot}Br_2]$ salt.[11] The even-n F_n^- ions presented in Figure 2 show branched structures of the lowest total energy states beginning with n = 10 and ending at n = 22 (Figures 3 and 4).

DOI: 10.1021/acs.jpca.5b02431
J. Phys. Chem. A 2015, 119, 6483−6492

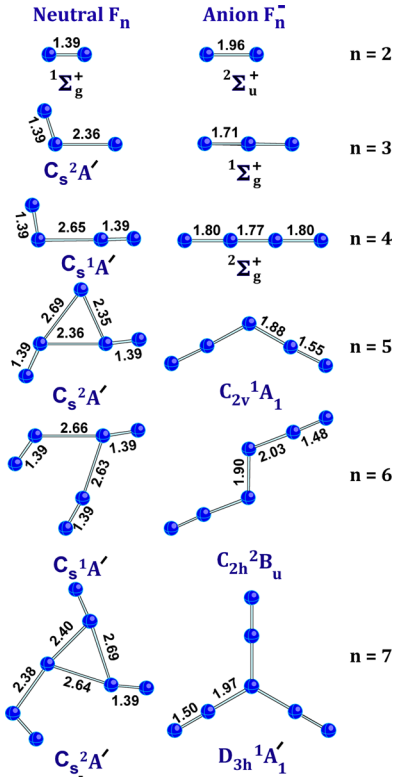

Figure 1. Geometrical structures of the lowest total energy states of F_n and F_n^- for n = 2−7 optimized using the CAM-B3LYP/6-311+G* method. Bond lengths are in ångstroms.

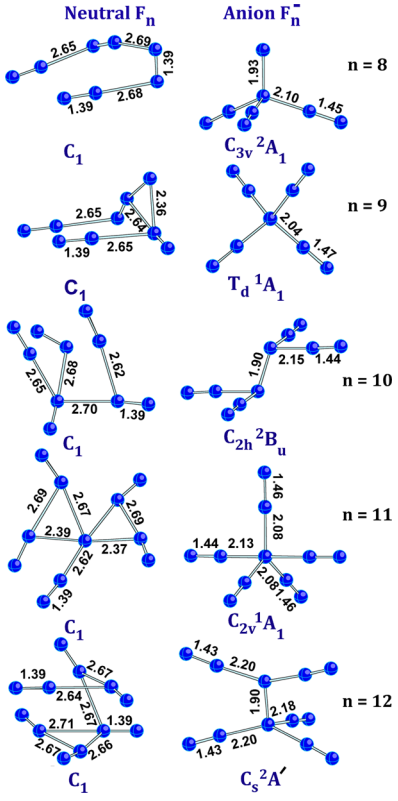

Figure 2. Geometrical structures of the lowest total energy states of F_n and F_n^- for n = 8−12 optimized using the CAM-B3LYP/6-311+G* method. Bond lengths are in ångstroms.

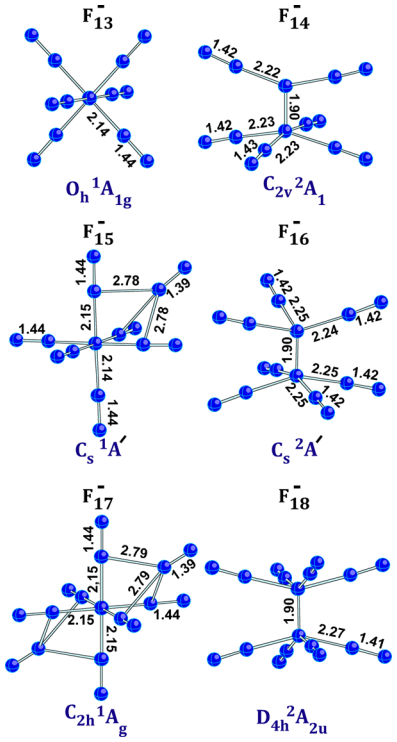

Figure 3. Geometrical structures of the lowest total energy states of F_n^- for n = 13−18 optimized using the CAM-B3LYP/6-311+G* method. Bond lengths are in ångstroms.

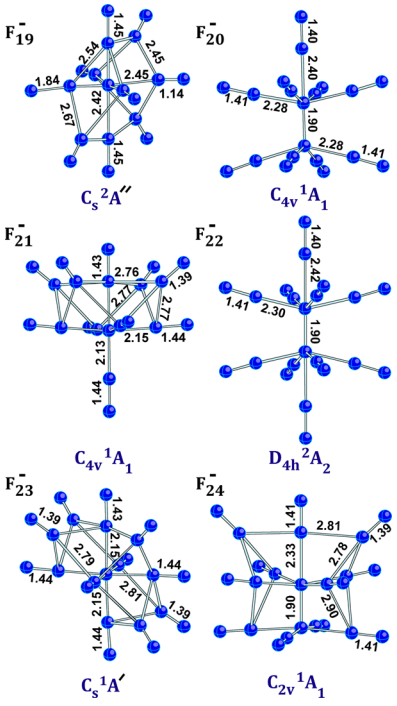

Figure 4. Geometrical structures of the lowest total energy states of F_n^- for n = 19−24 optimized using the CAM-B3LYP/6-311+G* method. Bond lengths are in ångstroms.

As is seen in Figures 1 and 2, geometrical structures of the neutral F_n are highly asymmetric. This is in contrast with the results of optimizations for $(N_2)_n$, whose geometrical structures have been found[61] to be near linear chains, and with the results of computations on $(O_2)_4$, which predicted a cyclic geometrical

DOI: 10.1021/acs.jpca.5b02431
J. Phys. Chem. A 2015, 119, 6483−6492

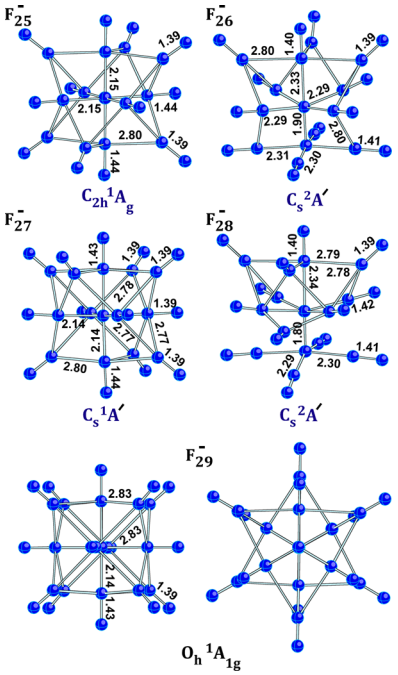

Figure 5. Geometrical structures of the lowest total energy states of F_n^- for n = 25−29 optimized using the CAM-B3LYP/6-311+G* method. Bond lengths are in ångstroms.

configuration.[62,63] We have optimized neutral isomers of F_n up to n = 29 to use their total energies in estimation of the corresponding adiabatic electron affinities, but only geometrical structures for the lowest total energy states of F_n up to n = 12 are shown in Figures 1 and 2. For larger n, there are a plenty of F_n isomers closely spaced in total energy whereas these neutral clusters are barely bound.

The lowest total energy state of the F_{13}^- ion possesses an octahedral geometrical structure displayed in Figure 3. The odd-n pattern in the formation of geometrical structures for n > 13 corresponds to the successive addition of a F_2 unit into the octants of the F_{13}^- frame. There are several options for a F_2 addition in the range of 15 < n < 27, all of which have been tested. It was found that the highest symmetry geometrical structures possible for a given n are preferred (Figures 3−5). All octants are occupied at n = 29, and the resulting geometrical structure possesses O_h symmetry. The even-n pattern corresponds to the successive addition of a F_2 unit to the central F_2 "dumbbell" beginning with F_{10}^- (C_{2h}) and ending at F_{22}^- (D_{4h}). The geometrical structures of F_{24}^-, F_{26}, and F_{28}^- are formed by successive adding of a F_2 unit into the top quadrants of F_{20}^-. That is, the latter pattern is similar to the odd-n pattern which starts at n = 15.

The building patterns in the neutral and anion series can also be described as follows. The neutrals with odd n are derived from the weak interactions of a F radical with a variable number of F_2 molecules. The neutrals with even n can be derived from the interactions of F_2 molecules with each other, which are even weaker (the calculated bond distances are around 2.65 Å whereas van der Waals radius value is ∼1.4 Å). The polyfluoride anions with odd n can be derived from a F^- anion interacting weakly with different numbers of F_2 molecules (up to 6 directly interacting F_2, followed by another 8 F_2 forming the secondary shell), except for F_3^-, which has somewhat stronger bonds. The polyfluoride anions with even n can be derived from the direct weak interaction of F_2^- with up to 10 F_2 molecules until one reaches F_{22}^- and then goes back to 9 directly bonded F_2 and 2, 3, and 4 secondarily bonded F_2 to reach F_{28}^-.

3.2. Electron Affinities and Ionization Energies.

Adiabatic electron affinities of neutral F_n computed according to eq 1 are presented in Figure 6. The values computed using

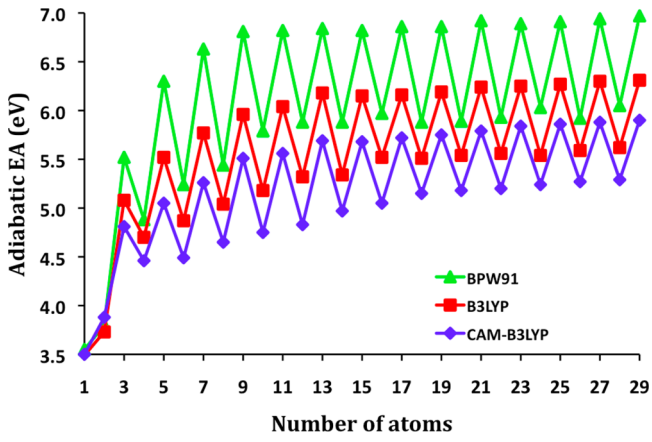

Figure 6. Adiabatic electron affinities (eV) of F_n for n = 1−29 computed at three levels of theory using the 6-311+G* basis set.

all three methods follow the same pattern: they grow as n increases and show remarkable odd−even-n oscillations with the larger values corresponding to odd n. This peculiarity can be related with the presence of a hole in the odd-n neutrals. As the simplest case, we consider a pair F_3−F_3^- whose geometrical configurations are presented in Figure 1. According to the natural bond analysis,[64] there is a single bond occupied by two electrons in the F_2 unit of F_3, whereas the third atom is attached by polarization forces. Not surprisingly, the F_2−F dissociation energy computed at the CAM-B3LYP/6-311+G(3df) level of theory is only 0.04 eV (∼1 kcal/mol). In this case, the hole is localized at the distant F atom. The attachment of an extra electron to F_3 results in a linear symmetric geometrical structure of the F_3^- anion where the atoms are held by the (4e, 3c) bond.[25,35] The F_3^- anion is stable with respect to dissociation via the $F_3^- \rightarrow F_2 + F^-$ decay channel by ∼1 eV.

It is interesting to note that the F_{n+1}^- species formed by adding of a F^- ion to a neutral F_n species is more stable than the neutral F_{n+1} formed after adding a neutral F atom to the same F_n neutral. Actually, there is a whole class of compounds possessing this property. Such compounds are described with a general formula MF_{k+1}, where k is the maximal formal valence of the central atom M, which have been named as superhalogens.[65] All superhalogens possess an electron affinity exceeding the electron affinities of a halogen atom. The maximal valence of a F atom ($2s^2 2p^5$) is seven; thus, the corresponding superhalogen should be F_9^- where the central atom is coordinated to eight ligand atoms. However, the ligands of F_9 are presented by F_2 dimers, as can be seen in Figure 2.

Since the EA_{ad} of F_3 exceeds the EA of a F atom (Table 1), one could admit in this case a weaker superhalogen formulation where k is the normal valence of M in MF_{k+1}. Both formulations do coincide for alkali atoms whose superhalogens are MF_2 (M = Li−Cs). Their superhalogen character has been confirmed by the results of CCSD(T) computations[66] using large basis sets. However, the real superhalogens should possess larger electron affinities. Indeed, the CCSD(T) EA_{ad} of LiF_2 is 5.45 eV whereas

DOI: 10.1021/acs.jpca.5b02431
J. Phys. Chem. A 2015, 119, 6483−6492

Table 3. Vertical Electron Detachment Energies of the F_n^- Anions F_2^- Computed by Using Different Methods[a]

Even-n F_n^-: Doublet → Singlet														
n =	2	4	6	8	10	12	14	16	18	20	22	24	26	28
CAM-B3LYP	6.14	7.34	6.15	6.29	7.27	7.38	6.58	7.58	7.67	7.72	7.77	7.73	7.81	7.82
B3LYP	6.11	7.18	7.48	6.88	7.64	7.71	7.76	7.84	7.89	7.93	7.96	7.94	8.00	8.01
BPW91	5.48	6.56	7.05	7.19	7.46	7.40	7.54	7.67	7.60	7.76	7.64	7.83	7.66	7.82
Even-n F_n^-: Doublet → Tripet														
n =	2	4	6	8	10	12	14	16	18	20	22	24	26	28
CAM-B3LYP	5.67	7.51	6.36	6.48	6.97	7.07	6.81	7.29	7.39	7.44	7.49	7.42	7.51	7.52
B3LYP	5.60	7.22	7.11	7.02	7.31	7.54	7.43	7.53	7.58	7.61	7.63	7.61	7.65	7.67
BPW91	5.05	6.35	6.88	7.11	7.41	7.53	7.41	7.66	7.68	7.63	7.61	7.65	7.83	7.85
Odd-n F_n^-: Singlet → Doublet														
n =	3	5	7	9	11	13	15	17	19	21	23	25	27	29
CAM-B3LYP	5.60	6.23	6.38	6.47	6.45	6.56	6.59	6.61	6.64	6.66	6.69	6.72	6.75	6.79
B3LYP	5.88	6.73	6.99	7.08	7.06	7.08	7.10	7.12	7.14	7.18	7.18	7.30	7.22	7.24
BPW91	5.81	6.63	7.07	7.34	7.37	7.42	7.44	7.45	7.47	7.51	7.49	7.51	7.52	7.63

[a]All values are in eV.

the EA_{ad} of F_3 computed at the CCSD(T)/6-311+G(3df) level of theory is 4.28 eV.

As can be seen in Figure 6, the EA_{ad} values grow steadily when n increases and exceed the electron affinity of a F atom except for F_2; therefore, all F_n (n = 3−29) are superhalogens. The EA_{ad} values computed by all three methods are quite different at a given n value, although the values computed using each method show similar trends as n increases. The long-range corrected CAM-B3LYP method consistently predicts a lower EA_{ad} for all n. For example, the EA_{ad} values for F_{29} are 5.90, 6.31, and 6.67 eV obtained using the CAM-B3LYP, B3LYP, and BPW91 methods, respectively. Because the CAM-B3LYP value of the EA_{ad} of F_3 is closer to the value computed at the CCSD(T) level of theory, we expect that the CAM-B3LYP values present more reliable estimates for larger n. The BPW91 EA_{ad} values appear to be overestimated to about the same extent as the values computed for F_2 and F_3 in Table 1.

Experimental measurements using photoelectron detachment spectroscopy produce the energies of vertical detachment of an extra electron from an anion. Theoretically, such energies can be obtained by computing the neutral total energies at the anion geometry. If the anion state with the spin multiplicity $2S+1$ is not a singlet state, then accessible final states can have spin multiplicities of $2S$ and $2S + 2$. If the anion is in a singlet state, then the final neutral state is a doublet. Therefore, we compute the vertical electron detachment energies, E_{VED}, using the total energies of the corresponding lowest total energy states for odd n as

$$E_{VED}(F_n^-) = E_{tot}^{el}(F_n,\text{doublet}) - E_{tot}^{el}(F_n^-,\text{singlet}) \quad (5)$$

and for even n as

$$E_{VED}(F_n^-) = E_{tot}^{el}(F_n,\text{singlet or triplet}) - E_{tot}^{el}(F_n^-,\text{doublet}) \quad (6)$$

The E_{VED} values computed according to these equations are presented in Table 3. As can be seen, the values computed by all methods show similar oscillations as the adiabatic electron affinities do except for irregularities at small values of odd n. The E_{VED} values obtained for transitions from the doublet anion state to final neutral triplet states are sometimes smaller than those obtained for transitions to singlet states. This is related to the fact that a F_n^- geometrical structure is completely different from the equilibrium geometry of the corresponding neutral F_n cluster, and a triplet state can be lower at the anion geometry than the lowest total energy singlet state. Optimizations of neutral singlet and triplet states performed for several cases where the E_{VED} values corresponding to transitions to the final triplet states are lower than those to the singlet states (e.g., F_{12}^-) have always resulted in a singlet state as the lowest total energy state.

3.3. Binding Energies. To gain insight into the thermodynamic stability of polyfluoride anions, we estimated energies of abstraction of F, F^-, F_2, and F_2^-. The energy of a F atom abstraction from a F_n^- anion is computed as

$$D_0(F_n^- \rightarrow F_{n-1}^- + F) = [E_{tot}^{el}(F_{n-1}^-) + E_0(F_{n-1}^-)] + E_{tot}^{el}(F) - [E_{tot}^{el}(F_n^-) + E_0(F_n^-)] \quad (7)$$

and the energy of a F_2 dimer abstraction is computed as

$$D_0(F_n^- \rightarrow F_{n-2}^- + F) = [E_{tot}^{el}(F_{n-2}^-) + E_0(F_{n-2}^-)] + [E_{tot}^{el}(F_2) + E_0(F_2)] - [E_{tot}^{el}(F_n^-) + E_0(F_n^-)] \quad (8)$$

The F^- and F_2^- abstraction energies have been computed using properly charge-modified eqs 7 and 8. The dissociation energies corresponding to four decay channels were computed at the CAM-B3LYP level of theory and are presented in Figure 7. As can be seen, the abstraction energies of a single F atom (a) show small-amplitude oscillations for smaller n and almost no deviation from the value of 0.75 eV at larger n. The energies corresponding to the $F_n^- \rightarrow F_{n-1} + F^-$ channel (b) are the largest in the dissociation series, whereas the abstraction of a neutral F_2 dimer (c) requires the smallest energy which oscillates around 0.1 eV. The energies corresponding to the $F_n^- \rightarrow F_{n-2} + F_2^-$ decay channel (d) are relatively large and exhibit an antiphase oscillating character with respect to the energies of channel (b).

The abstraction energies computed at the B3LYP and BPW91 levels of theory show similar small positive values. For example, the F_2 abstraction energies for F_{29}^- are 0.10, 0.07, and 0.03 eV computed using the CAM-B3LYP, B3LYP, and BPW91 methods, respectively. To stress the bound character of the F_n^-, we present in Figure 8 energies of formation from $[(n-2)/$

DOI: 10.1021/acs.jpca.5b02431
J. Phys. Chem. A 2015, 119, 6483−6492

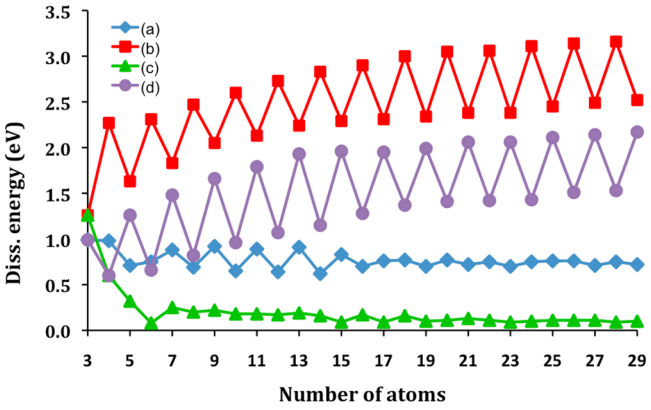

Figure 7. Dissociation energies (eV) of polyfluoride anions via the channels (a) $F_n^- \rightarrow F_{n-1}^- + F$; (b) $F_n^- \rightarrow F_{n-1} + F^-$; (c) $F_n^- \rightarrow F_{n-2}^- + F_2$; (d) $F_n^- \rightarrow F_{n-2} + F_2^-$ computed at the CAM-B3LYP/6-311+G* level of theory.

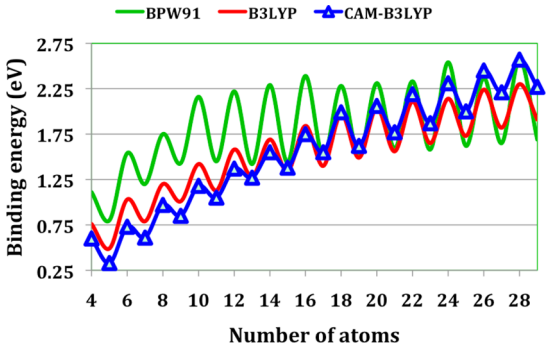

Figure 8. Formation energies from F_2 and a single F_2^- anion for even-n F_n^- and from F_2 and a single F_3^- anion for odd-n F_n^-.

$2]F_2$ and one F_2^- for even n and from $[(n-2)/2]F_2$ and F_3^- for odd n computed using all three methods. These energies are computed for even n as

$$E_{\mathrm{dim}}(n) = \frac{n-2}{2}[(E_{\mathrm{tot}}^{\mathrm{el}}(F_2) + E_0(F_2)] + [(E_{\mathrm{tot}}^{\mathrm{el}}(F_2^-) + E_0(F_2^-)] - [E_{\mathrm{tot}}^{\mathrm{el}}(F_n^-) + E_0(F_n^-)] \quad (9)$$

and for odd n as

$$E_{\mathrm{dim}}(n) = \frac{n-2}{2}[(E_{\mathrm{tot}}^{\mathrm{el}}(F_2) + E_0(F_2)] + [(E_{\mathrm{tot}}^{\mathrm{el}}(F_3^-) + E_0(F_3^-)] - [E_{\mathrm{tot}}^{\mathrm{el}}(F_n^-) + E_0(F_n^-)] \quad (10)$$

As can be seen in Figure 8, the formation energies steadily grow independent of the method used and show oscillating character. An even-n anion is more stable than its odd-n neighbors. Note that the CAM-B3LYP formation energy as a function of n is nearly linear for odd- and even-n sets. The largest variations show the values computed using the BPW91 method, although they are in qualitative agreement with the values computed using two other methods. Neutral formation energies are appreciably smaller. For example, the CAM-B3LYP energy of the F_{28} formation from F_2 is 0.60 eV, i.e., only 0.04 eV per dimer. The B3LYP and BPW91 methods predict smaller formation energies of 0.24 and 0.07 eV, respectively. That is, the F_n neutrals are bound by polarization forces, which is in agreement with the experimental data obtained in solid and liquid states of fluorine.[67,68]

3.4. Diagrams of Molecular Orbitals. To gain insight into the bonding nature of F_n^-, we have chosen the tetrahedral F_9^- anion as a representative for the odd-n moiety and the branched F_{10}^- anion as a representative for the even-n moiety. The valence molecular orbitals of F_9^- are presented in Figure 9.

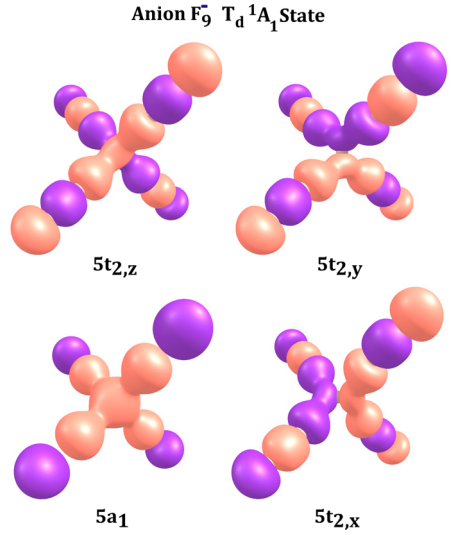

Figure 9. Bonding molecular orbitals of the F_9^- anion.

There are four bonding orbitals involving the central atom of a_1 and t_2 symmetry. In this anion, the extra electron is distributed between the central atom (~0.46 e) and four outer atoms of the F_2 ligands (~0.14 e on each atom) whereas the internal F atoms of the F_2 ligands carry no charge.

The F_{10}^- anion has an odd number of electrons and its ground state is a doublet. In the unrestricted DFT variant used in this work, there are bonding orbitals in both spin representations, which are not necessarily identical. The bonding orbitals of the F_{10}^- anion are presented in Figure 10. As can be seen, the bonding orbitals in both spin representations possess similar shapes but possess different contributions from atomic orbitals.

4. SUMMARY

Among polyhalides, the most studied are polyiodide I_n^- anions whose structures are known for n = 3–29. On the contrary, polyfluorine F_n^- anions are the least studied polyhalide anions and only F_3^- has been observed experimentally. To gain insight into the structure of polyfluorines, we performed computations on neutral and singly charged F_n in the same range of $3 \leq n \leq 29$. For calibration purposes, we tested first the dependence of computed electron affinities of F and F_2 as well as dissociation energies of F_2^- and F_3^- on the method and basis set used. We selected 12 methods belonging to 4 different groups and two basis sets. Three methods, namely, BPW91 (GGA-DFT), B3LYP (HF-DFT), and CAM-B3LYP (long-range corrected HF-DFT) and along with the 6-311+G* basis set of triple-ζ quality have been chosen for the rest of calculations.

The neutral F_n species are barely bound and each species possesses plenty of states with asymmetric geometrical structures that are nearly degenerate in total energy for n > 4. On the contrary, the F_n^- anions possess symmetric

DOI: 10.1021/acs.jpca.5b02431
J. Phys. Chem. A 2015, 119, 6483–6492

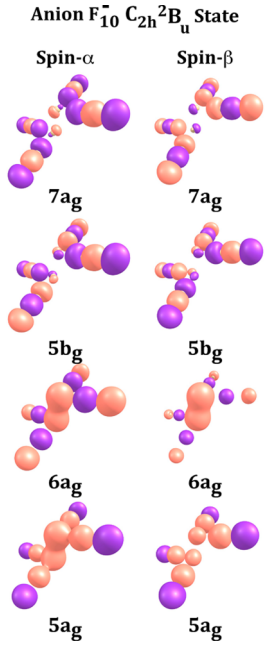

Figure 10. Bonding molecular orbitals of the F_{10}^- anion.

geometrical structures that include a tetrahedron (F_9^-) and octahedrons (F_{13}^- and F_{29}^-). The patterns in the geometrical structures as n grows are different in odd-n and even-n series. No formation of linear F_3 units is found; the construction pattern consists of adding a F_2 dimer to the preceding geometrical structure in both odd-n and even-n series.

Adiabatic electron affinities of F_n possess an oscillating behavior as a function of n. The larger EA_{ad} values correspond to odd n-values which can be related to the presence of a hole on a F atom in these cases. For $n \geq 3$, the smallest EA_{ad} value of 4.58 eV belongs to F_4 and the largest EA_{ad} value of 5.90 eV belongs to F_{29}, as computed at the CAM-B3LYP level; that is, all EA_{ad} values are larger than the EA of a F atom (3.40 eV). Therefore, all F_n for $n \geq 3$ are superhalogens.

The abstraction of F, F^-, and F_2^- from the F_n^- anions require fairly large energies but barely 0.1 eV is required for the abstraction of a neutral F_2 dimer. This property could be very useful if salts $[X]^+[F_n]^-$ were synthesized. Such salts would dissociate at fairly low temperatures yielding large amounts of F_2 and could serve as highly effective biocide agents.

AUTHOR INFORMATION

Corresponding Author

*G. L. Gutsev. E-mail: gennady.gutsev@famu.edu. Phone: +1-850-599-3815.

Notes

The authors declare no competing financial interest.

ACKNOWLEDGMENTS

Portions of this research were conducted with high performance computational resources provided by the Louisiana Optical Network Initiative (http://www.loni.org). This research has also used resources of the National Energy Research Scientific Computing Center, a DOE Office of Science User Facility supported by the Office of Science of the U.S. Department of Energy under Contract No. DE-AC02-05CH11231. P.J. acknowledges support of the U.S. Department of Energy, Office of Basic Energy Sciences, Division of Materials Sciences and Engineering under Award # DE-FG02-96ER45579.

REFERENCES

(1) Haller, H.; Riedel, S. Recent Discoveries of Polyhalogen Anions − from Bromine to Fluorine. *Z. Anorg. Allg. Chem.* **2014**, *640*, 1281−1291.

(2) Svensson, P. H.; Kloo, L. Synthesis, Structure, and Bonding in Polyiodide and Metal Iodide-Iodine Systems. *Chem. Rev.* **2003**, *103*, 1649−1684.

(3) Tebbe, K.-F.; Buchem, R. The Most Iodine-Rich Polyiodide Yet: Fc_3I_{29}. *Angew. Chem., Int. Ed. Engl.* **1997**, *36*, 1345−1346.

(4) Otsuka, K.; Mori, H.; Kikuchi, H.; Takano, K. Density Functional Theory Calculations of Iodine Cluster Anions: Structures, Chemical Bonding Nature, and Vibrational Spectra. *Comput. Theor. Chem.* **2011**, *973*, 69−75.

(5) Groessl, M.; Fei, Z.; Dyson, P. J.; Katsyuba, S. A.; Vikse, K. L.; McIndoe, J. S. Mass Spectrometric and Theoretical Study of Polyiodides: The Connection between Solid State, Solution, and Gas Phases. *Inorg. Chem.* **2011**, *50*, 9728−9733.

(6) Wolff, M.; Okrut, A.; Feldmann, C. $[(Ph)_3PBr][Br_7]$, $[(Bz)(Ph)_3P]_2[Br_8]$, $[(n\text{-}Bu)_3MeN]_2[Br_{20}]$, $[C_4MPyr]_2[Br_{20}]$, and $[(Ph)_3PCl]_2[Cl_2I_{14}]$: Extending the Horizon of Polyhalides via Synthesis in Ionic Liquids. *Inorg. Chem.* **2011**, *50*, 11683−11694.

(7) Vitske, V.; Herrmann, H.; Enders, M.; Kaifer, E.; Himmel, H.-J. Wrapping an Organic Reducing Reagent in a Cationic Boron Complex andIts Use in the Synthesis of Polyhalide Monoanionic Networks. *Chem. - Eur. J.* **2012**, *18*, 14108−14116.

(8) Alhanash, F. B.; Barnes, N. A.; Godfrey, S. M.; Khan, R. Z.; Pritchard, R. G. Generation of a high symmetry 2D-polybromide network in the structure of $\{[(o\text{-}SCH_3C_6H_4)_3PBr][Br]\cdot 0.5(\mu\text{-}Br_2)3\}_n$. The templating effect of the C_3 symmetric $[(o\text{-}SCH_3C_6H_4)_3PBr]^+$ cation. *Polyhedron* **2013**, *65*, 102−109.

(9) Haller, H.; Ellwanger, M.; Higelin, A.; Riedel, S. Structural Proof for a Higher Polybromide Monoanion: Investigation of $[N(C_3H_7)_4][Br_9]$. *Angew. Chem., Int. Ed.* **2011**, *50*, 11528−11532.

(10) Haller, H.; Ellwanger, M.; Higelin, A.; Riedel, S. Z. Investigation of Polybromide Monoanions of the Series $[NAlk_4][Br_9]$ (Alk =Methyl, Ethyl, Propyl, Butyl). *Z. Anorg. Allg. Chem.* **2012**, *638*, 553−558.

(11) Haller, H.; Schröder, J.; Riedel, S. Structural Evidence for Undecabromide $[Br_{11}]^-$. *Angew. Chem., Int. Ed.* **2013**, *52*, 4937−4940.

(12) Taraba, J.; Zdirad Zak, Z. Diphenyldichlorophosphonium Trichloride−Chlorine Solvate 1:1, $[PPh_2Cl_2]^+Cl_3^-\cdot Cl_2$: An Ionic Form of Diphenyltrichlorophosphorane. Crystal Structures of $[PPh_2Cl_2]^+Cl_3^-\cdot Cl_2$ and $[(PPh_2Cl_2)^+]_2[InCl_5]_2^-$. *Inorg. Chem.* **2003**, *42*, 3591−3594.

(13) Gutsev, G. L. Structures of CCl_n^- and Cl_n^- Anions (n = 1- 4) According to Results of Local Density Functional Calculations. *J. Phys. Chem.* **1991**, *95*, 5773−5783.

(14) Gutsev, G. L. The Structure and Stability of Cl_n^- Clusters, n = 2−7. *Chem. Phys.* **1991**, *156*, 427−437.

(15) Brückner, R.; Haller, H.; Ellwanger, M.; Riedel, S. Polychloride Monoanions from $[Cl_3]^-$ to $[Cl_9]^-$: A Raman Spectroscopic and Quantum Chemical Investigation. *Chem. - Eur. J.* **2012**, *18*, 5741−5747.

(16) Schlöder, T.; Riedel, S. Investigation of Heterodimeric and Homodimeric Radical Cations of the Series: $[F_2O_2]^+$, $[F_2Cl_2]^+$, $[Cl_2O_2]^+$, $[F_4]^+$, and $[Cl_4]^+$. *RSC Adv.* **2012**, *2*, 876−881.

(17) Nizzi, K. E.; Pommerening, C. A.; Sunderlin, L. S. Gas-Phase Thermochemistry of Polyhalide Anions. *J. Phys. Chem. A* **1998**, *102*, 7674−7679.

(18) Thanthiriwatte, K. S.; Spruell, J. M.; Dixon, D. A.; Christe, K. O.; Jenkins, H. D. B. Structures, Vibrational Frequencies, and Stabilities of Halogen Cluster Anions and Cations, $X_n^{+/-}$, n = 3, 4, and 5. *Inorg. Chem.* **2014**, *53*, 8136−8146.

(19) Christe, K. O.; Bau, R.; Zhao, D. X-ray Crystal Structure and Raman Spectrum of Tribromine (1+) Hexaf luoroarsenate(V), $Br_3^+AsF_6^-$, and Raman Spectrum of Pentabromine(1+)

DOI: 10.1021/acs.jpca.5b02431
J. Phys. Chem. A 2015, 119, 6483−6492

Hexafluoroarsenate(V), $Br_5^+AsF_6^-$. *Z. Anorg. Allg. Chem.* **1991**, *593*, 46−60.
(20) Gutsev, G. L.; Boldyrev, A. I. DVM-Xα Calculations on the Ionization Potentials of MX_{k+1}^- Complex Anions and the Electron Affinity of MX_{k+1} "Superhalogens". *Chem. Phys.* **1981**, *56*, 277−283.
(21) Ponikvar-Svet, M.; Edwards, K. F.; Liebman, J. F. An Overview of the Understanding of Ions Containing Solely Fluorine Atoms. *Acta Chim. Slov.* **2013**, *60*, 471−483.
(22) Cahill, P. A.; Clifford, E.; Dykstra, C. E.; Martin, J. C. The Structure and Stability of the 10-F-2 Trifluoride Ion, a Compound of a Hypervalent First Row Element. *J. Am. Chem. Soc.* **1985**, *107*, 6359−6362.
(23) Novoa, J. J.; Mota, F.; Alvarez, S. Structure and Stability of the X_3^- Systems (X = F, Cl, Br). *J. Phys. Chem.* **1988**, *92*, 6561−6566.
(24) Ewig, C. S.; Van Wazer, J. R. Ab Initio Studies of Molecular Structures and Energetics. 4. Hexacoordinated NF_6^- and CF_6^{2-} Anions. *J. Am. Chem. Soc.* **1990**, *112*, 109−114.
(25) Kar, T.; Marcos, E. S. Three-Center Four-Electron Bonds and Their Indices. *Chem. Phys. Lett.* **1992**, *192*, 14−20.
(26) Heard, G. L.; Marsden, C. J.; Scuseria, G. E. The Trifluoride Anion, F_3^-. A Difficult Challenge for Quantum Chemistry. *J. Phys. Chem.* **1992**, *96*, 4359−4366.
(27) Gutsev, G. L. A Theoretical Study on the Structure and Stability of the PF_n and PF_n^- Series (n = 1 - 6). J. *J. Chem. Phys.* **1993**, *98*, 444−452.
(28) Wright, T. G.; Lee, E. P. F. Ab initio Studies of X_3^- (X = F, Cl). *Mol. Phys.* **1993**, *79*, 995−1009.
(29) Malcolm, N. O. J.; McDouall, J. J. W. Combining Multi-configurational Wave Functions with Density Functional Estimates of Dynamic Electron Correlation. *J. Phys. Chem.* **1996**, *100*, 10131−10134.
(30) Tozer, D. J.; Sosa, C. P. The Alkali Metal Trifluorides $M^+F_3^-$: How Well Can Theory Predict Experiment? *Mol. Phys.* **1997**, *90*, 515−524.
(31) Ogawa, Y.; Takahashi, O.; Kikuchi, O. J. Ab Initio MO Study of Structure and Sstability of X_3 (X = F, Cl, Br, I) in Solution. *J. Mol. Struct.: THEOCHEM* **1998**, *424*, 285−292.
(32) Tuinman, A. A.; Gakh, A. A.; Hinde, R. J.; Compton, R. N. The First Direct Observation of the Trifluoride Anion (F_3^-) in the Gas Phase. *J. Am. Chem. Soc.* **1999**, *121*, 8397−8398.
(33) Christe, K. O. On the Instability of Salts Containing the Ttrifluoride Anion. *J. Fluorine Chem.* **1995**, *71*, 149−150.
(34) Mota, F.; Novoa, J. J. The Symmetry Breaking Problem in the Triflouride Anion: A Multireference Approach. *J. Chem. Phys.* **1996**, *105*, 8777−8784.
(35) Braïda, B.; Hiberty, P. C. What Makes the Trifluoride Anion F_3^- So Special? A Breathing-Orbital Valence Bond ab Initio Study. *J. Am. Chem. Soc.* **2004**, *126*, 14890−14898.
(36) Braïda, B.; Hiberty, P. C. Application of the Valence Bond Mixing Configuration Diagrams to Hypervalency in Trihalide Anions: A Challenge to the Rundle-Pimentel Model. *J. Phys. Chem. A* **2008**, *112*, 13045−13052.
(37) Czernek, J.; Živný, O. The Multiconfigurational-Reference Internally Contracted Configuration Interaction/ Complete Basis Set Study of the Excited States of the Trifluoride Anion F_3^-. *J. Chem. Phys.* **2008**, *129*, 194305.
(38) Riedel, S.; Köchner, T.; Wang, X.; Andrews, L. Polyfluoride Anions, a Matrix-Isolation and Quantum-Chemical Investigation. *Inorg. Chem.* **2010**, *49*, 7156−7164.
(39) Krishnan, R.; Binkley, J. S.; Seeger, R.; Pople, J. A. Self-Consistent Molecular Orbital Methods. XX. A Basis Set for Correlated Wave Functions. *J. Chem. Phys.* **1980**, *72*, 650−654.
(40) Becke, A. D. Density-Functional Exchange-Energy Approximation With Correct Asymptotic-Behavior. *Phys. Rev. A: At., Mol., Opt. Phys.* **1988**, *38*, 3098−3100.
(41) Perdew, J. P.; Wang, Y. Accurate and Simple Analytic Representation of the Electron-Gas Correlation-Energy. *Phys. Rev. B: Condens. Matter Mater. Phys.* **1992**, *45*, 13244−13249.
(42) Perdew, J. P.; Burke, K.; Ernzerhof, M. Generalized Gradient Approximation Made Simple. *Phys. Rev. Lett.* **1996**, *77*, 3865−3868.
(43) Perdew, J. P.; Kurth, S.; Zupan, A.; Blaha, P. Accurate Density Functional with Correct Formal Properties: A Step Beyond the Generalized Gradient Approximation. *Phys. Rev. Lett.* **1999**, *82*, 2544−2547.
(44) Tao, J. M.; Perdew, J. P.; Staroverov, V. N.; Scuseria, G. E. Climbing the Density Functional Ladder: Nonempirical Meta-Generalized Gradient Approximation Designed for Molecules and Solids. *Phys. Rev. Lett.* **2003**, *91*, 146401.
(45) Perdew, J. P.; Ruzsinszky, A.; Csonka, G. I.; Constantin, L. A.; Sun, J. Workhorse Semilocal Density Functional for Condensed Matter Physics and Quantum Chemistry. *Phys. Rev. Lett.* **2009**, *103*, 026403.
(46) Becke, A. D. Density-Functional Thermochemistry. 3. The Role of Exact Exchange. *J. Chem. Phys.* **1993**, *98*, 5648−5652.
(47) Grimme, S. Semiempirical Hybrid Density Functional with Perturbative Second-Order Correlation. *J. Chem. Phys.* **2006**, *124*, 034108.
(48) Vydrov, O. A.; Scuseria, G. E. Assessment of a Long Range Corrected Hybrid Functional. *J. Chem. Phys.* **2006**, *125*, 234109.
(49) Vydrov, O. A.; Heyd, J.; Krukau, A.; Scuseria, G. E. Importance of Short-Range Versus Long-Range Hartree-Fock Exchange for the Performance of Hybrid Density Functionals. *J. Chem. Phys.* **2006**, *125*, 074106.
(50) Vydrov, O. A.; Scuseria, G. E.; Perdew, J. P. *J. Chem. Phys.* **2007**, *126*, 154109.
(51) Yanai, T.; Tew, D.; Handy, N. A New Hybrid Exchange-Correlation Functional Using the Coulomb-Attenuating Method (CAM-B3LYP). *Chem. Phys. Lett.* **2004**, *393*, 51−57.
(52) Chai, J.-D.; Head-Gordon, M. Long-Range Corrected Hybrid Density Functionals with Damped Atom-Atom Dispersion Corrections. *Phys. Chem. Chem. Phys.* **2008**, *10*, 6615−6620.
(53) Bartlett, R. J.; Musial, M. Coupled-Cluster Theory in Quantum Chemistry. *Rev. Mod. Phys.* **2007**, *79*, 291−352.
(54) Frisch, M. J.; Trucks, G. W.; Schlegel, H. B.; Scuseria, G. E.; Robb, M. A.; Cheeseman, J. R.; Scalmani, G.; Barone, V.; Mennucci, B.; Petersson, G. A.; et al. *Gaussian 09*, Revision C.01; Gaussian, Inc.: Wallingford, CT, 2009.
(55) Feller, D.; Peterson, K. A. Re-examination of Atomization Energies of the Gaussian-2 Set of Molecules. *J. Chem. Phys.* **1999**, *110*, 8384−8396.
(56) Kozuch, S.; Martin, J. M. L. Halogen Bonds: Benchmarks and Theoretical Analysis. *J. Chem. Theory Comput.* **2013**, *9*, 1918−1931.
(57) Forni, A.; Pieraccini, S.; Rendine, S.; Sironi, M. Halogen Bonds with Benzene: An Assessment of DFT Functionals. *J. Comput. Chem.* **2014**, *35*, 386−394.
(58) Gutsev, G. L.; Bauschlicher, C. W., Jr. Electron Affinities, Ionization Energies, and Fragmentation Energies of Fe_n Clusters (n = 2−6): A Density Functional Theory Study. *J. Phys. Chem. A* **2003**, *107*, 7013−7023.
(59) Pichierri, F. Structure and Bonding in Polybromide Anions $Br^-(Br_2)_n$ (n = 1−6). *Chem. Phys. Lett.* **2011**, *515*, 116−121.
(60) Walbaum, C.; Richter, M.; Sachs, U.; IPantenburg, I.; Riedel, S.; Mudring, A.-V.; Meyer, G. Iodine−Iodine Bonding makes Tetra-(diiodine)chloride, $[Cl(I_2)_4]^=$, Planar. *Angew. Chem., Int. Ed.* **2013**, *52*, 12732−12735.
(61) Owens, F. J. Prediction of Unusual Curled Nitrogen Oligomers. *Chem. Phys. Lett.* **2014**, *593*, 20−23.
(62) Forte, G.; Angilella, G. G. N.; March, N. H.; Pucci, R. The Nuclear Structure and Related Properties of Some Low-Lying Isomers of Free-Space O_n Clusters (n = 6, 8, 12). *Phys. Lett. A* **2013**, *377*, 801−803.
(63) Ochoa-Calle, A. J.; Ramírez-Solís, A. On the Stability of the Cyclic O_8 Molecule. *Chem. Phys. Lett.* **2014**, *592*, 326−329.
(64) Reed, A. E.; Curtiss, L. A.; Weinhold, F. Intermolecular Interactions From a Natural Bond Orbital, Donor-Acceptor Viewpoint. *Chem. Rev.* **1988**, *88*, 899−926.

DOI: 10.1021/acs.jpca.5b02431
J. Phys. Chem. A 2015, 119, 6483−6492

(65) Gutsev, G. L.; Boldyrev, A. I. The Theoretical Investigation of the Electronic Affinity of Chemical Compounds. *Adv. Chem. Phys.* **1985**, *61*, 169−221.
(66) Gutsev, G. L.; Bartlett, R. J.; Boldyrev, A. I.; Simons, J. Adiabatic Electron Affinity of Small Superhalogens: LiF_2, $LiCl_2$, NaF_2, and $NaCl_2$. *J. Chem. Phys.* **1997**, *107*, 3867−3875.
(67) Legasov, V. A.; Makeev, G. N.; V.F. Sinyansky, V. F.; Smirnov, B. M. Fluorine Absorption Spectra and Some Fluorides in Condensed State. *J. Fluorine Chem.* **1978**, *11*, 109−118.
(68) Jacob, E.; Goubeau, J. Die Schwingungsspektren des Flüssigen Fluors. *Ber. Bunsen-Ges. Phys. Chem.* **1970**, *74*, 992−994.
(69) Hotop, H.; Lineberger, W. C. Binding Energies in Atomic Negative Ions: II. *J. Phys. Chem. Ref. Data* **1985**, *14*, 731−750.
(70) Blondel, C.; Cacciani, P.; Delsart, C.; Trainham, R. High-Resolution Determination of the Electron Affinity of Fluorine and Bromine using Crossed Ion and Laser Beams. *Phys. Rev. A: At., Mol., Opt. Phys.* **1989**, *40*, 3698−3701.
(71) Andersen, T.; Haugen, H. K.; Hotop, H. Binding Energies in Atomic Negative Ions: III. *J. Phys. Chem. Ref. Data* **1999**, *28*, 1511−1533.
(72) Chupka, W. A.; Berkowitz, J.; Gutman, D. Electron Affinities of Halogen Diatomic Molecules as Determined by Endoergic Charge Transfer. *J. Chem. Phys.* **1971**, *55*, 2724−2733.
(73) Wenthold, P. G.; Squires, R. R. Bond Dissociation Energies of F_2^- and HF_2^-. A Gas-Phase Experimental and G2 Theoretical Study. *J. Phys. Chem.* **1995**, *99*, 2002−2005.
(74) Chupka, W. A.; Berkowitz, J. Kinetic Energy of Ions Produced by Photoionization of HF and F_2. *J. Chem. Phys.* **1971**, *54*, 5126−5132.
(75) Artau, A.; Nizzi, K. E.; Hill, B. T.; Sunderlin, L. S.; Wenthold, P. G. Bond Dissociation Energy in Trifluoride Ion. *J. Am. Chem. Soc.* **2000**, *122*, 10667−10670.

DOI: 10.1021/acs.jpca.5b02431
J. Phys. Chem. A 2015, 119, 6483−6492